Comparison between point and long gauge FBG based strain sensors during a railway bridge load test.

Abstract.

Strain is a key parameter in laboratory and bridge load testing. The selection of a strain sensor depends on several factors, including the aim of the test and the specimen material. The application of the right sensor is vital to obtain accurate readings, especially in the case of heterogeneous materials such as concrete. This paper focuses on long gauge and point FBG based strain sensors and their possible applications. First, strain sensors are described, after which long gauge and point FBG strain sensors are compared in a concrete specimen test, a concrete column test and static and dynamic tests on a concrete railway bridge.

1. Introduction

The aim of SHM is to develop systems that provide information on significant damage to or relative changes in a structure. In many geotechnical and civil engineering applications its use is fundamental in order to: 1) monitor the safety level in real time, 2) determine whether the actual behavior is the same as the designed behavior, and 3) optimize maintenance work.

Obtaining these objectives requires the use of sensors installed in the structure to provide information on important parameters regarding its state. Mechanical deformation is one of the parameters that provide most information on the state of the material [1]. The information obtained includes the mechanical strain applied to the material and different sensor installation strategies can give information on the forces to which the structural element is subjected.

Deformation can be measured by a number of different technologies, one of the most advanced being fiber optic sensors, due to their advantages over other types of sensor and the fact that their prices have dropped in recent years [1, 2, 3]. The choice of sensor type largely depends on the purpose of the monitoring and the type of material in which the deformation is to be measured ([2], [4]).

The fiber optic sensors used to measure deformation can be divided into *distributed* and *discrete*. The former measure the deformation of the material along a length of fiber and give the values at all its points, while the latter measure deformation between two points. The distance between these two points is known as *gage length* and defines the length of the sensor.

Regarding sensor gage length: discrete sensors are classified into *short* or *long* gage. The traditional electric strain gauges belong to the first group and measure the deformation between two points quite close to each other (within several millimeters), so that the values they give are strongly influenced by local defects and irregularities in the study zone. This type of sensor is suitable for monitoring homogeneous materials such as steel.

On the other hand, materials such as concrete, wood, stone or compounds such as el CFRP (Carbon Fiber Reinforced Polymer) may contain local defects or irregularities such as cracks, spalling or hollows. Such materials need to be monitored by long sensors [2], which are not affected by local irregularities (the sensor gives the average deformation value between the two points). Sensor lengths can vary between a few centimeters and several meters and they can be embedded in a structure under construction (as in the case of concrete structures) or be attached to already existing surfaces, wooden surfaces and historical structures.

Measures R. [5] proposed that the difference in length between the point sensor and long-gage sensor should be no more than 50 mm. This division may be acceptable for homogeneous materials like steel or non- homogeneous materials with very short distances between irregularities and fine cracks, as in mortar. However, this criterion cannot be applied to other non-homogeneous materials such as concrete, in which the aggregate size can reach 32 mm and there may be 100 or 200 mm between two consecutive cracks.

It is therefore impossible to establish the limit between point and long-gage sensors, since this will depend on the properties of the material to be studied. For example, a sensor 50 mm long could be regarded as long-gage if applied to steel, but would be a point sensor when applied to concrete.

Glisic [6] provided guidelines for the selection of an appropriate gage length, and tables to estimate errors. For example, in the case of a beam made of non-homogeneous material with a constant cross-section, length L_{beam} and depth h, the best gage length L_s of the sensor would have to be almost 10 L_c, the latter being the distance between two consecutive irregularities. Studies exist ([7], [8], [9], [10]) on the behavior of concrete elements and mixed materials in which the 50 mm long strain gages used to measure concrete deformation provided satisfactory results.

In this context, this paper compares the behavior of point and long-gage FBG sensors in cases in which the results are expected to be similar (compression stresses only). The sensors were first installed on a concrete specimen and in a concrete column compression load test and a railway bridge load test. In all the cases, the point FBG sensors used were developed by Torres et al [11] and the long-gage FBG sensors were provided by a commercial manufacturer [12].

A comparison is made of the results of static and dynamic loading tests on a railway bridge with prefabricated concrete beams by means of a point gage fiber optic sensor and a 1 m long-gage fiber optic sensor attached at the same position on the bridge. The bridge had only one 23.5 m long span. Both sensors were fitted to the underside of one of two central beams in the center section to measure deformation during the application of static and dynamic loads.

The paper is organized as follows: Section 2 describes the different types of fiber optic sensors used for monitoring structures. Section 3 describes the principles on which they operate and gives the principal characteristics of the sensors used in the study. Sections 4 and 5 describe the experimental tests, the results obtained and include a critical analysis of the same. The conclusions are given in Section 6.

From the results obtained in the study it can be said that although it is advisable to use long-gage sensors when monitoring heterogeneous materials, there may also be situations in which this may not be strictly necessary.

1. Long-gage sensors vs. point sensors

The measures obtained from long-gage and point sensors are in general different due to the different information that each one provides. Point sensors give information on the deformation and behavior of the structure at a specific point, while the long-gage gives the value of mean deformation along its length, which is attributed to the sensor's mid-point.

In heterogeneous materials, a long-gage sensor may pass through various irregularities and this will influence both the reading and its interpretation (Fig.1). Eq.(1) shows that for a sensor of length A to B, the measured deformation $\varepsilon_{C,s}$ depends on the distribution of deformations $\varepsilon_{x,s}(x)$ between points A and B, on the number and magnitude of the irregularities $\Delta w_{d,i}$ (e.g. cracks, hollows, etc.) between A and B, and sensor length l_s :

$$\varepsilon_{C,s} = \frac{\Delta L_s}{L_s} = \frac{u_B - u_A}{x_B - x_A} = \frac{1}{L_s}\int_{x_A}^{x_B} \varepsilon_{x,s}(x)\,\mathrm{d}x + \frac{1}{L_s}\sum_i \Delta w_{d,i} \tag{1}$$

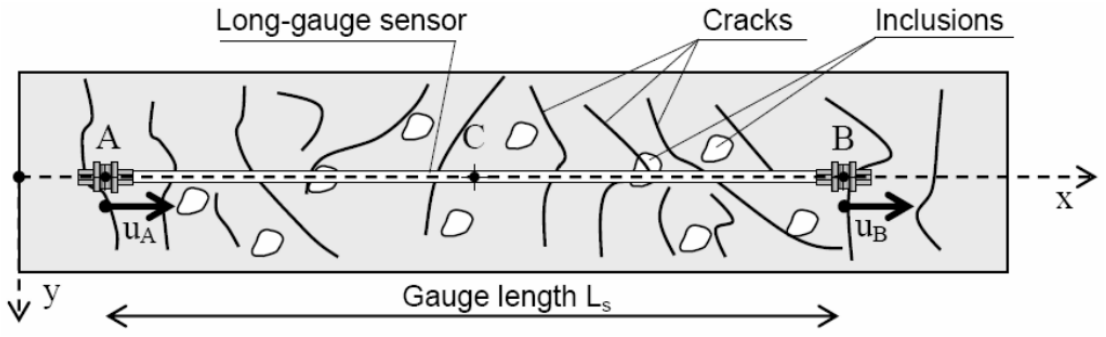

Figure 1. Scheme of a long-gauge sensor in a heterogeneous material (Reproduced from [2]).

The length of a point sensor may be several times less than or equal to the distance between irregularities in the material being studied, which means their readings are strongly influenced by local defects and cannot be interpreted as valid for the material as a whole.

A long-gauge sensor by definition has a length several times greater than the maximum distance between irregularities or the maximum diameter of any added materials. For example, for concrete, a long-gauge sensor must be several times longer than the maximum distance between cracks or than the diameters of any hollows. Their principal advantage is that although they measure average deformation over a certain distance, they are not influenced by local irregularities or added materials. Their readings thus give information relative to the material's behavior on a scale that could be regarded as homogeneous.

Therefore, the division between long-gage and point sensors basically depends on the differences in the properties of the materials forming thestructure, although other factors such as the installation process or price may have to be considered when choosing which type to use.

The working of a fiber optic sensor requires that, whatever principle it is based on (Bragg gratings, interferomtery, etc) or installation (embedded or fixed to the surface) the fiber must be pres-stressed if it is to measure compression deformation correctly, as if not it may warp even under small compression loads. Almost all long-gage sensors presently available (e.g.[12], [13], [14], [15], [16]) are pre-stressed and generally give good results in different applications ([1], [2], [17], [18], [19]). However, pre-stressing is a delicate operation that requires at least two people and the following conditions: 1) the pre-stressing may be lost (the fiber can slip from its anchorage, temperature variations, etc.) and cause erroneous readings; 2) the pre-stress level may not be known; and 3) the fiber may break during the pre-stressing operation.

It is also possible that the installation of deformation sensors involves interference with the structure, e.g. it may require holes to be drilled to fix clamps, and this could be a problematic aspect: 1) from the point of view of durability of structures in aggressive environments, e.g. near the sea; and 2) in strongly reinforced concrete structures, since it is highly likely that the installation process will come into contact with the reinforcing, which means new holes will have to be drilled to place the sensor at another site.

The final factor to be considered is the financial aspect; long-gage sensors can be up to eight times more expensive than point sensors.

2. *Operating principle*

The working principle of the both sensors used (point and long gage) is based on the FBG (Fiber Bragg Grating).

A FBG is a reflector built in a short segment of the core of an optical fiber by exposing the fiber to an intense UV light. This exposure creates periodic alterations in the index of refraction of the fiber core, known as Bragg gratings, and makes the FBG (1) reflect only particular narrowband light wavelengths of light known as Bragg wavelengths, and (2) transmit all others (Fig 2).

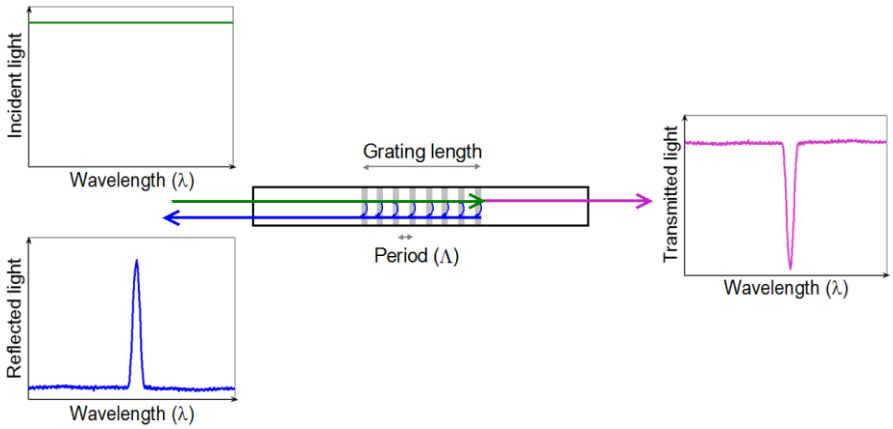

Fig. 2. Basic Bragg grating-based sensor system with transmissive or reflective detection options. Source: [20]. Reproduced bykind permission of the authors.

The Bragg wavelength condition is given by Eq. (2), where λ_B is the wavelength of the FBG, n_{eff} is the effective refractive index of the fiber core, and $\Lambda$is the Bragg grating period or distance between two consecutive alterations of the fiber core [11].

$$\lambda_B = 2\, n_{eff}\Lambda \tag{2}$$

External perturbations can result in strain (ε) and temperature (T) changes that modify the Bragg grating period Λ and also induce a shift $\Delta\lambda_B$ in the Bragg wavelength. This shift is given by Eq. 3, when only the dominant linear effects of $\varepsilon$and T on a FBG are considered and higher order cross-sensitivities are neglected (see [21] for more details).

$$\frac{\Delta\lambda_B}{\lambda_B} = k_\varepsilon \Delta\varepsilon + k_T \Delta T \tag{3}$$

In Eq. 7, $K_\varepsilon$and K_T are the coefficients of wavelength sensitivity to strain and temperature for a FBG. Their values are given by Eq. 4 and Eq. 5.

$$k_\varepsilon = \left[1 - 0.5\, n_{eff}\left(\rho_{12} - \upsilon(\rho_{11} - \rho_{12})\right)\right] \tag{4}$$

$$k_T = [1 + \xi] \tag{5}$$

where ρ_{11} and ρ_{12} are the components of the fiber optic strain tensor, υ is the fiber Poisson's ratio, $\xi$is the fiber thermo-optic coefficient and n_{eff} is the refractive index of the fiber (see [21,22] for more details).

3. Comparison of the readings of point and long-gage sensors. Preliminary studies.

4.1.Compression test on prismatic mass concrete specimens with a 0.10 m x 0.10 m cross section and 0.40 m height

The tests were carried out in the laboratory of the Concrete Science and Technology Institute (ICITECH in Spanish) of the Universitat Politècnica de València (UPV). The specimens were tested in an ICON press with an automatic control system and a maximum load of 2500 kN, connected to a computer system for data capture and storage.

The 0.3m long gauge sensor was mounted on the surface of the concrete specimen, as shown in Figure 3, fixed at both ends by a two-component adhesive. The specimens were submitted to a load-unload cycle. Point fiber optic sensors developed by Torres et al. [11] were placed alongside the long-gage optical sensors in the tests to compare the results obtained.

The interrogation system used for the deformation instrumentation was an FBG type MicronOptics, Model sm125-500 and a laptop computer with software developed specifically for this application in LabVIEWTM V. 8.5 programming language. The sm125-500 optical sensing interrogator is composed of a tunable Fabry-Perot laser source with a wavelength range of 1510 to 1590 nm and four optical channel outputs. Maximum data capture frequency is 1 Hz and measurement precision is 1 pm. The laptop used in the tests was an Intel Pentium 4 a 2.4 GHz with 768 MB Ram.

Load cells were used to record the loads applied by the hydraulic jack. This data was handled in real time by a Pentium IV computer. The data acquisition equipment was a Hewlett Packard Model HP 3852 and the acquisition software was programmed in LabVIEWTM.

The strain values measured by the reference point optic sensor were compared to those recorded by the long-gage sensor.

Figure 3. Concrete specimen.

Figure 4 gives the values of the experimental strains in concrete $\varepsilon_{P,EXP}$ as measured by the point sensor and those measured by the long gage sensor $\varepsilon_{LG,EXP}$ (non-continuous blue and black lines, respectively). Finally, the continuous maroon-colored line indicates the proposed load-unload cycle, with a maximum load value of 225 kN.

The results confirm that the differences between the readings of both sensors are almost negligible (below 3 % of the strain measured).

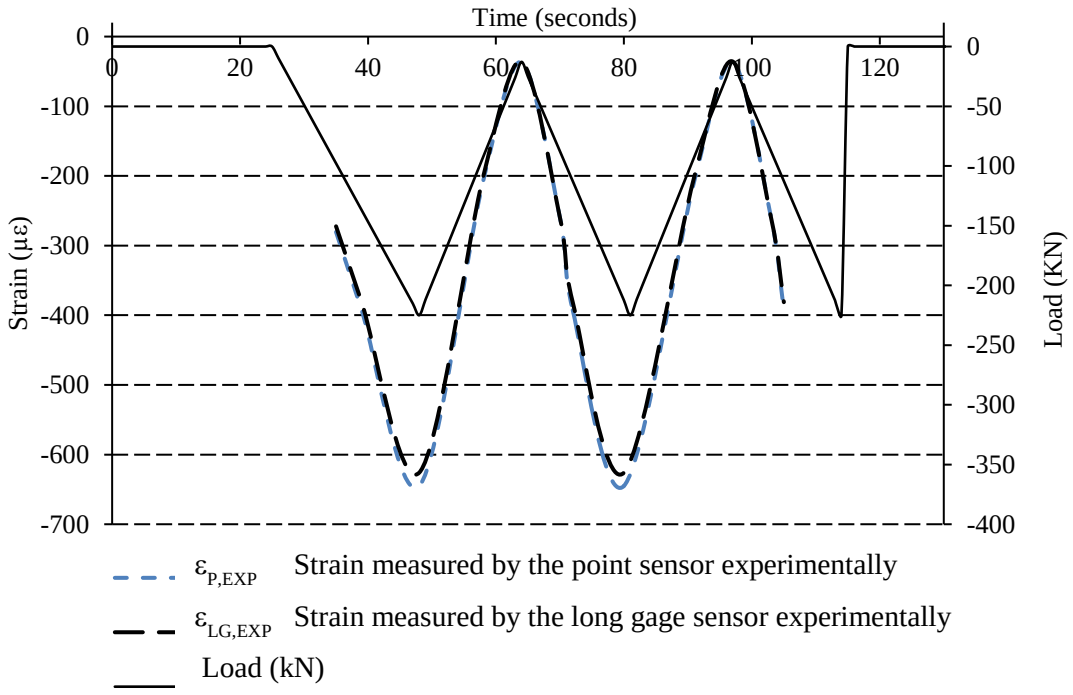

Figura 4. Experimental results of a simple compression test on a 0.4 high specimen monitored with point and long gage sensors.

3.1. Compression test on concrete column specimens with a 0.30 m x 3.00 m cross section and 3.00 m height.

Specimens were tested in another metal frame 3.5 m high and 5000 kN maximum load. As in the preceding case, the columns were placed on supports considered to be infinitely stiff and a vertical load was applied to the head until failure.

The 1 m long gage sensor was mounted on the surface of the concrete specimen, as shown in Figure 5, fixed at both ends by a two-component adhesive. The specimens were submitted to a load cycle. The data acquisition system was the same used for the previous test.

Figure 5. Concrete specimen.

Figure 6 gives the values of the experimental strains in concrete $\varepsilon_{P,EXP}$ measured by the point sensor and those measured by the long gage sensor $\varepsilon_{LG,EXP}$. Finally, the dot line indicates the proposed load cycle, with a maximum load value of 2000 kN.

The results confirm that the differences between the readings of both sensors are almost negligible (below 4 % of the strain measured).

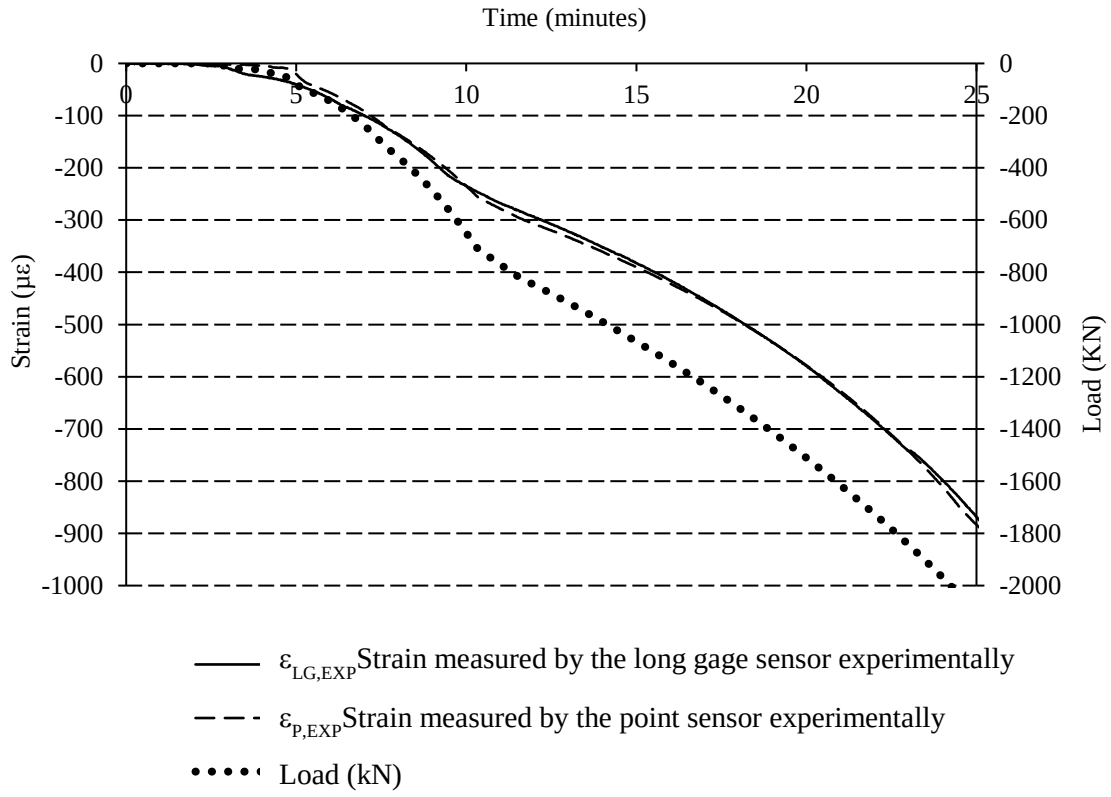

Figura 6. Experimental results of a simple compression test on a 3 m high column monitored with point and long gage sensors.

4. *Case study*

After the preliminary laboratory test, the behavior of point and long gage sensors was compared on a static and dynamic load test on a 23,5 m long single-span railway bridge. The point and long-gage sensors were fitted to the underside of one of the beams at the center of the bridge.

4.1. Characteristics of the bridge used in the case study

The Moneder Gulley Bridge crosses the Benidorm/Denia railway line 57 km outside Benidorm. The bridge's construction project involved a total length of 23.5 m formed by a 22 m span between supports, plus two additional lengths of 0.75 m to reach the abutment (see Fig. 7)

Figure 7. The Moneder Gulley Bridge.

The deck is 5 m wide, formed by 4 1.30 m thick prefabricated prestressed beams supporting a 0.25 m thick slab. The beams have a double-T wide-flange cross section (60 cm x 195 cm, lower and upper flanges, respectively) and are coupled together in pairs with a distance of 1.05 m between axes, with a lateral cantilever of 0.4 m in the form of a prefabricated concrete shell used as formwork for casting the outer sections of the slab. The beams were prestressed to resist a compression stress of the order of 24.6 MPa in the bottom flange.

The deck covers a single straight span built over buttresses reinforced with concrete beams cast *in situ* and anchored to the terrain by micropiles. These concrete beams are 70 cm thick, of which 16 cm are embedded in the buttress to compensate for the slope. The beams are 1.20 m wide. There are two rows of 7 180 mm micropiles for each buttress.

The deck length is 22 m and total beam lengths are between 23.50 m and 23.58 m. The upper slab has outer sections 0.75 m wide, which leave a central zone of 3.5 m with a 40 cm layer of ballast, on which the rails are bedded.

The deck consists of a single span supported on neoprene bearing pads that do not restrict rotation, so that isostatic behavior is considered.

As can be seen in Figure 7, the distance between the underside of the deck and the upper surface of the railway line is 2.20 m, distributed as follows:

- Prefabricated beams: 1.30 m.
- Slab 0.25 m.
- Ballast: 0.30 m.
- Concrete sleepers: 0.20 m
- Rail 54 kg/m: 0.15 m

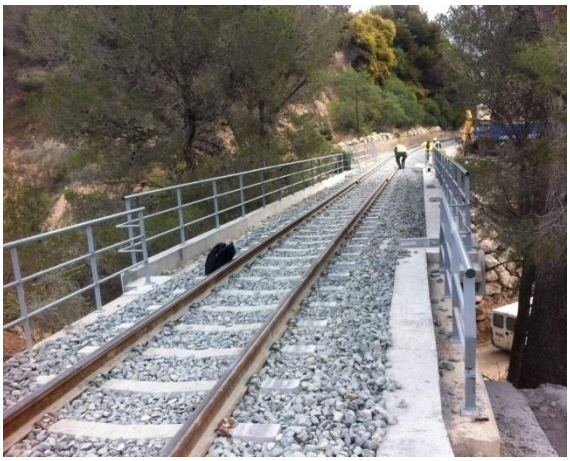

(a)

(b)

(c)

Figure 8. (a) – View of the bridge deck. (b) – Elastomeric bearing pads below one of the beams. (c) – View of the underside of the bridge from one of the stirrups.

4.2. Sensors

Long-gage and point deformation sensors were fitted to one of the central beams in the bridge center section. As the readings of both sensors required thermal compensation, a thermal sensor was installed close to the point deformation sensor. The long-gage sensor had already been fitted with a temperature compensation fiber.

a) Long-gauge deformation sensor

A FOS&S [12] (Figure 9) long-gauge sensor was used for the test.

(a) (b)

Figure 9. (a) - Installation of long-gage sensor. b) - Anchorage.

The sensor was anchored to the beam by two clamps. For correct operation, the sensor must be equipped with a pre-stressed fiber in order to measure compression strain. Pre-stressing is a delicate operation and should be carried out while monitoring the pre-stress level of the sensor, which depends on the expected deformations in the structure. Its value should be: 1) higher than the expected maximum compressive strain deformation and 2) lower than the maximum permitted by the sensor.

After drilling the holes in the structure, the sensor should be anchored at one end and the other end is allowed to deform by means of a nut and wrench system until the required level is reached (see Fig.10).

Figure 10. Installing the sensor.

This sensor measured 1 m between both anchorages and contained two optic fibers, one of which measured deformation while another helicoidal fibre measured the temperature variations required to carry out thermal compensation. As this is a helicoidal fiber, its length does not vary and it therefore is not affected by variations in deformation.

The temperature measured by this fiber is given by Eq.(6)

$$T = 22.5\ ℃ - \frac{S_1}{2\,S_2} + \sqrt{\left(\frac{S_1}{2\,S_2}\right)^2 + \frac{1}{S_2}\,ln\left(\frac{\lambda_{low}}{\lambda_{T,ref}}\right)} \tag{6}$$

T being the temperature in ºC, λ_{low} the wavelength of the temperature-measuring fiber, S_1 and S_2 two calibration parameters of the sensor with values of 6.07 $10^{-6}℃^{-1}$ and 9.2 $10^{-9}℃^{-2}$ respectively and $\lambda_{T,ref}$ is the value of the reference wavelength 1550.048 nm

When the temperature is known, the value of the mechanical strain is given by Eq.(7):

$$\Delta\varepsilon = \frac{1}{A\,L_o}\,ln\left(\frac{\lambda_{high}}{\lambda_{high,0}}\right) + \left[\frac{B}{L_o} + C\right](T - T_o) \tag{7}$$

$\Delta\varepsilon$ being the variation of mechanical strain of the structure expressed in με, L_o the distance between anchorage points, λ_{high} the wavelength of the deformation-measuring fiber, $\lambda_{high,0}$ the reference wavelength that coincides with the wavelength indicated by the sensor immediately after installation, T the temperature obtained from Eq.(2) and T_o the sensor's reference temperature immediately after installation, A, B and C sensor calibration parameters with values of 8.51 $10^{-7}\mu m^{-1}$, -21.11 $^{\mu m}/_{℃}$, y 15.9 $^{\mu\varepsilon}/_{℃}$, respectively.

b) Point temperature sensor

This was an FBG based temperature sensor designed by Torres [23]. Figure 11 shows the sensor before being fixed to the structure at a distance of 1 cm from the deformation point sensor.

Figure 11. Point temperature sensor.

The temperature is obtained from Eq.(8) as described in the preceding sub-section.

c) Point deformation sensor

d)

The point sensor used in the tests was designed by Torres et al. [11]. It was enclosed in a polyester resin sheath and fixed to the structure by means of a bicomponent adhesive (Fig.12).

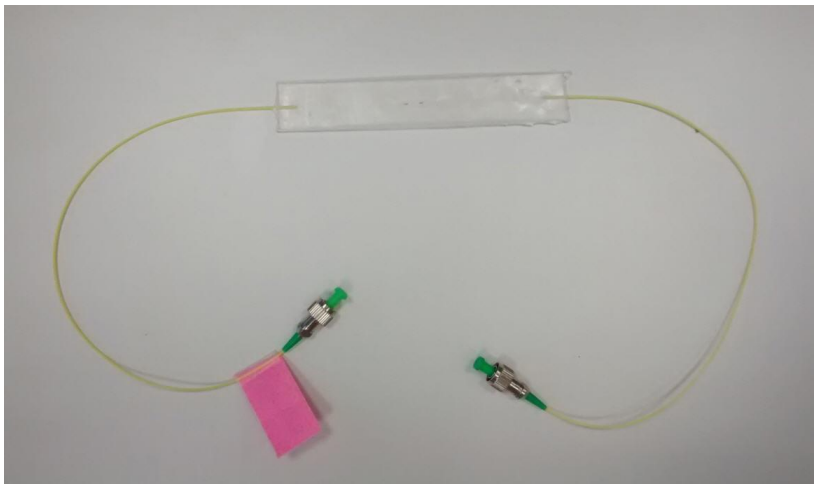

Figure 12. Point deformation sensor.

Details of the sensor configuration, installation process and adhesive properties can be found in [11]. A fine layer of adhesive was spread on the base of the sensor, which was initially held to the structure by adhesive tape (see Fig.13). The thickness of the layer of adhesive is critical to obtain correct readings. This is normally around 400 μm and transmits approximately 99% of the deformations between the structure and the sensor [11].

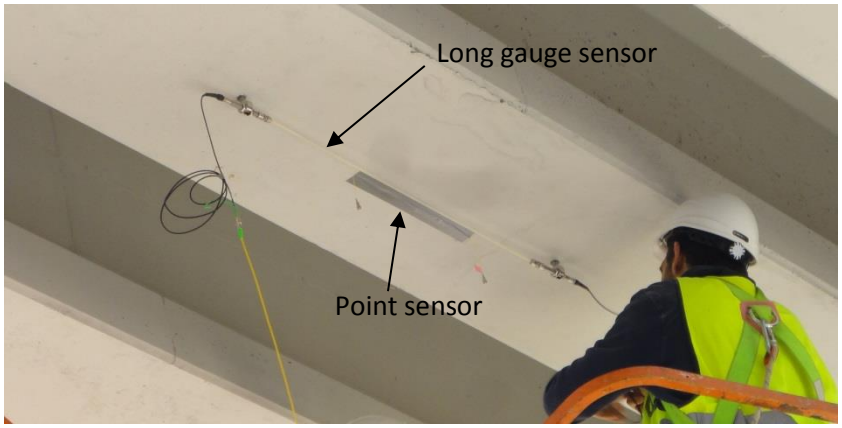

Figure 13. Long-gage point sensor fitted to the underside of a beam.

The temperatures must also be monitored to obtain the thermal compensation for the deformation readings. The temperature and deformation variations are obtained from Eqs.(8) and (9) as described in 11]:

$$\Delta T = \frac{1}{K_{T2}}\left(\frac{\Delta\lambda_{B2}}{\lambda_{B2}}\right) \tag{8}$$

$$\Delta\varepsilon = \frac{1}{K_{\varepsilon}}\left(\frac{\Delta\lambda_{B1}}{\lambda_{B1}}\right) - \frac{K_{T1}}{K_{\varepsilon}\,K_{T2}}\left(\frac{\Delta\lambda_{B2}}{\lambda_{B2}}\right) \tag{9}$$

where K_{ε} is the sensitivity of the optic fibre to deformation at a value of 1.15 $^{pm}/_{\mu\varepsilon}$, K_{T1} is sensitivity to the temperature of the fiber adhered to the concrete at a value of 17.5 $^{pm}/_{\circ C}$, K_{T2}

sensitivity of the optic fiber to temperature at a value of 8 $^{pm}/_{°C}$. All these coefficients were obtained experimentally.

4.3. Interrogator unit and software.

A *MicronOptics sm125* [15] interrogation system was used for the static load test and a laptop computer with software developed specifically for this application in *LabVIEW*^{TM} V. 8.5 programming language.

For the dynamic load test, the interrogator system used was a *MicronOpticssm130-700* [15]and the same laptop and software used for static test. This interrogator has a maximum data scan frequency of 1KHz. The sm130-700 optical sensing interrogator is composed of a tunable *Fabry-Perot* laser source with a wavelength range of 1510 to 1590 nm and four optical channel outputs. Measurement repeatability is 1 pm. The laptop used in the tests was an Intel Pentium 4 a 2.4 GHz with 768 MB Ram.

4.4. Train used in the test

To carry out the test a 2500 Series diesel train that covers the Benidorm/Denia route was used.

Total weight of an empty 2500 Series train is 558.4 KN (fully loaded is 662.4 KN) divided among four twin-axle bogeys (see Figure 14) with a total length of 34.79 m.

(a)

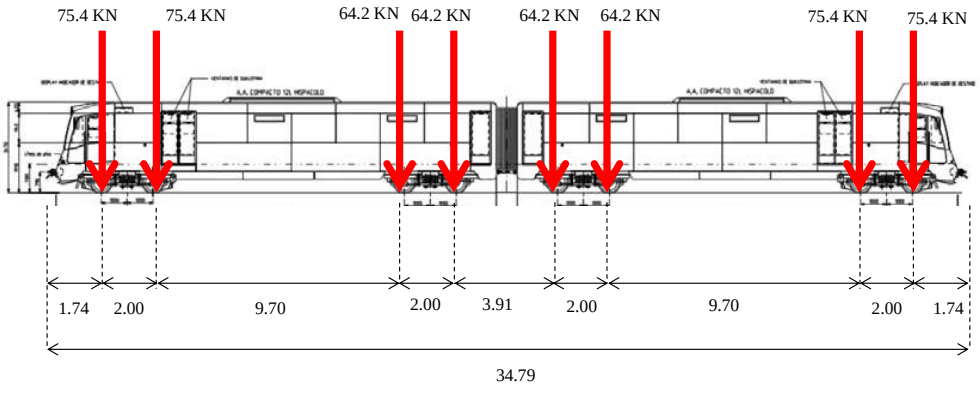

(b)

Figure 14. (a) – 2500 Series diesel train used for the load test. (b) – Axle loads.

4.5. Loading hypotheses considered

Two types of load test were carried out:

- A static test consisting of a single load hypothesis that involved placing the train in a symmetrical position in relation to the central point of the bridge span (see Fig.15). This position is shown in Figure 10, with the mid-point of the train situated at the center of the bridge at 5.62 m from the center of the abutment.
- The speed of the train was kept at 2-3 km/hour when being positioned to avoid the appearance of dynamic effects.
- A dynamic test in which the train passed at a speed of 50 km/hour, the maximum permitted when crossing the bridge.

The theoretical effect of the loads on the bridge in both tests was calculated. It was found that the increase in the maximum strain on the lower flange of the concrete in the static test was Δfc = -1.19 MPa (positive compression). The theoretical strain on this flange before the test was fp = 17.85 MPa, the resulting minimum strain on this lower flange is of the order of 16.66 MPa. It can therefore be seen that the minimum resulting strain on the lower flange was positive, and that it later became compressed, so that no cracks were indicated during the tests.

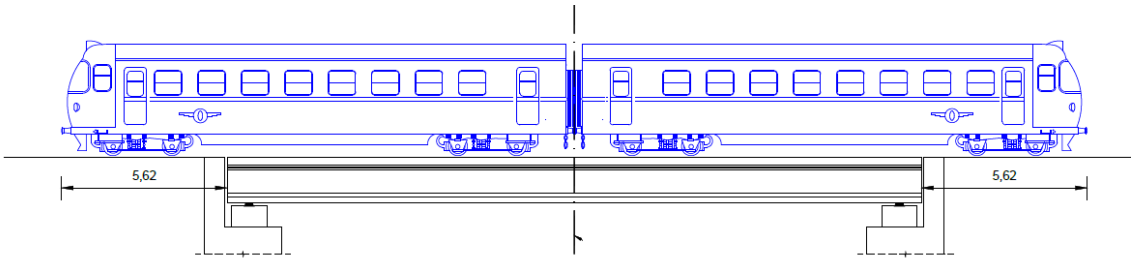

(a) Source: [24]

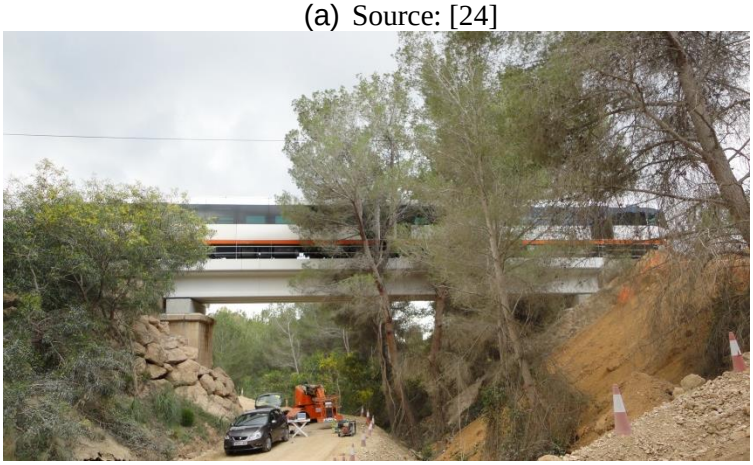

(b)

Figure 15. Static load test. Position of the train on the bridge.

4.6. Result

Temperature readings

Temperature variations were recorded at the center of the span near the sensors during the static load test and were not found to have experienced brusque changes in this period.

As can be seen in Figure 16, the temperature readings given by the sensors are quite low (around 1º C) and describe practically the same tendency.

Temperature variations in general have a strong effect on the sensors installed in the structure. Even though these variations are quite small, they were taken into account in the subsequent data processing.

The temperature variations during the dynamic load test are not shown due to the short duration of the test (less than one minute).

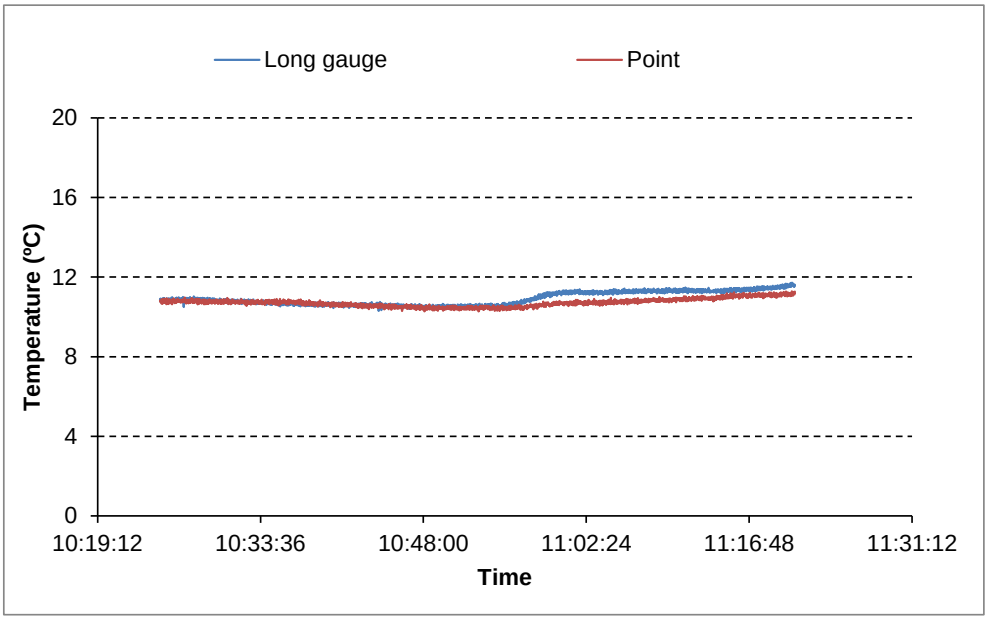

Figure 16. Temperatures at the center of the span as read by the compensation sensor of the long-gage sensor and the point temperature sensor.

Deformation readings: static load test.

Figure 17 shows the evolution of both deformation sensors fixed to the center of the span. The load process at around 10:26:15 can be seen together with the evolution of deformation during the time the load was being put into position. When the load had been placed in the position indicated in Figure 15, deformation remained practically constant and stable. During loading, the passing of one of the bogeys of the first carriage can be seen to cause a slight reduction of the deformations (Fig.17a).

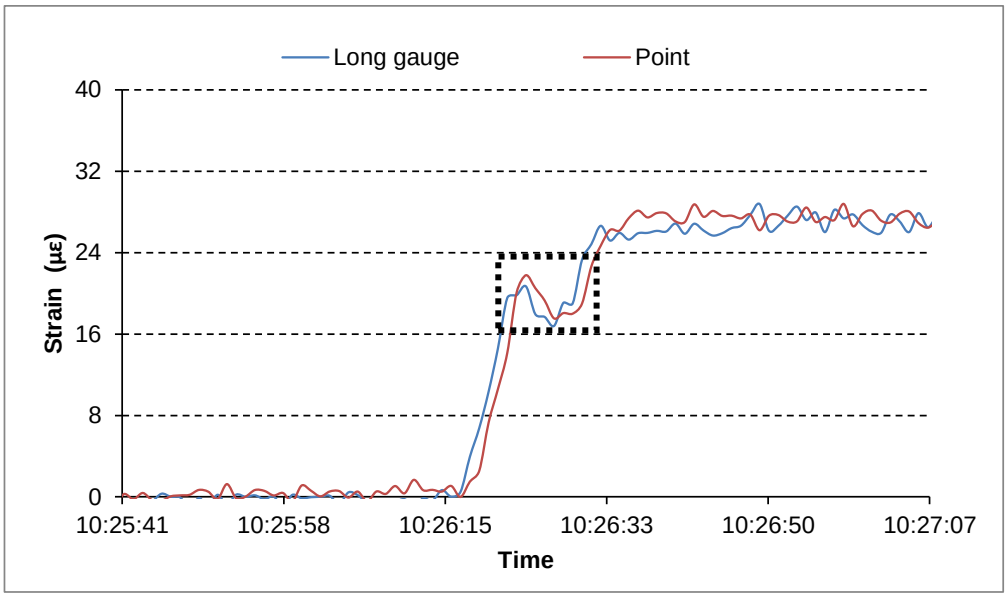

(a)

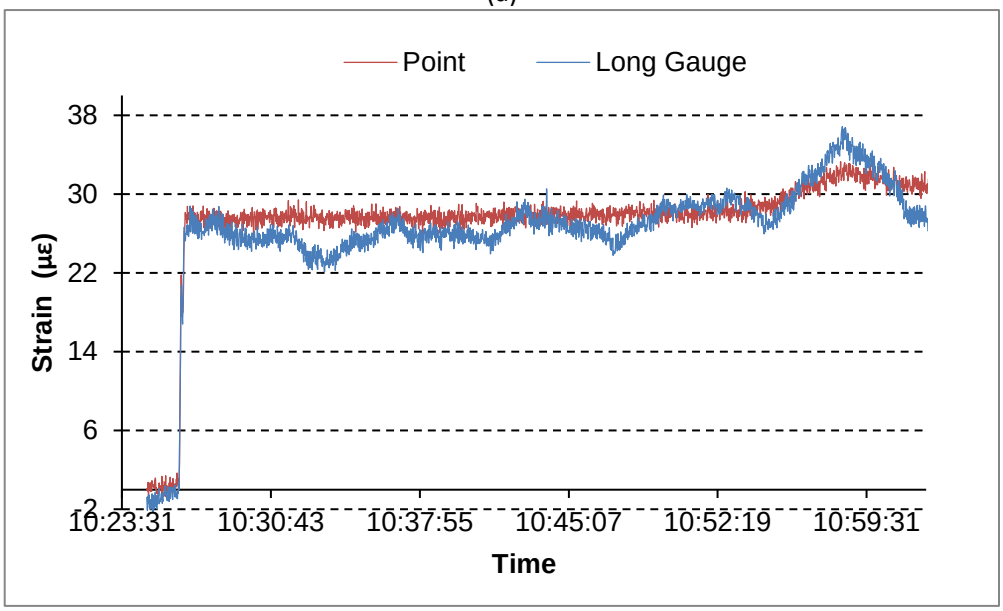

(b)

Figur 17. Evolution of deformation in long-gage and point sensors. (a) – Loading process. (b) – Complete test.

Figure 18 gives deformation evolution during unloading, during which the same speed was maintained as in loading (2-3 km/hour) to avoid dynamic effects.

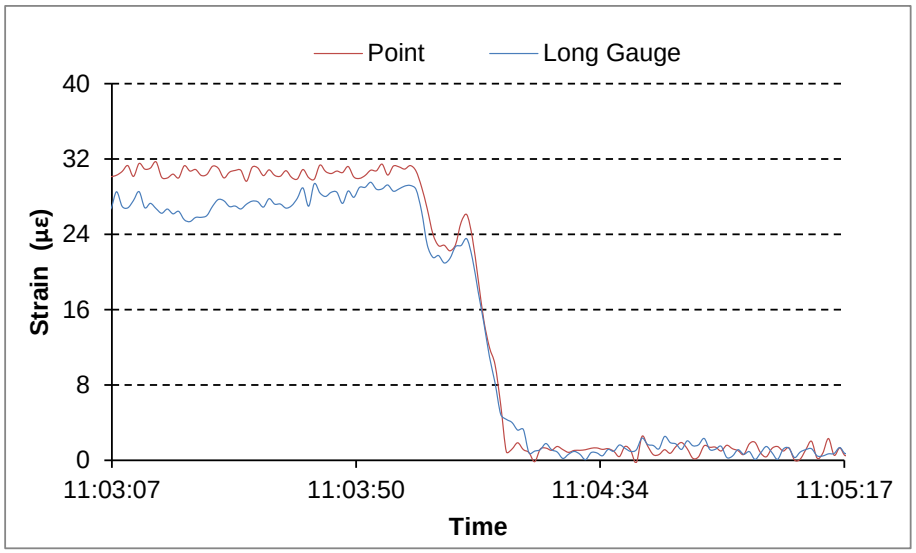

Figure 18. Deformation during the unloading process.

The maximum difference of the deformations measured by both sensor types during the static test is 3.2 με, which comprises 11.8 % of the measured increase in deformation. There is clearly a small difference in the measurements.

Deformation readings: dynamic load test.

Figure 19 shows deformation evolution in both sensors fixed to the center of the span when the train was crossing the bridge at the maximum permitted speed of 50 km/hour in the dynamic load test. The sampling frequency is 100 Hz.

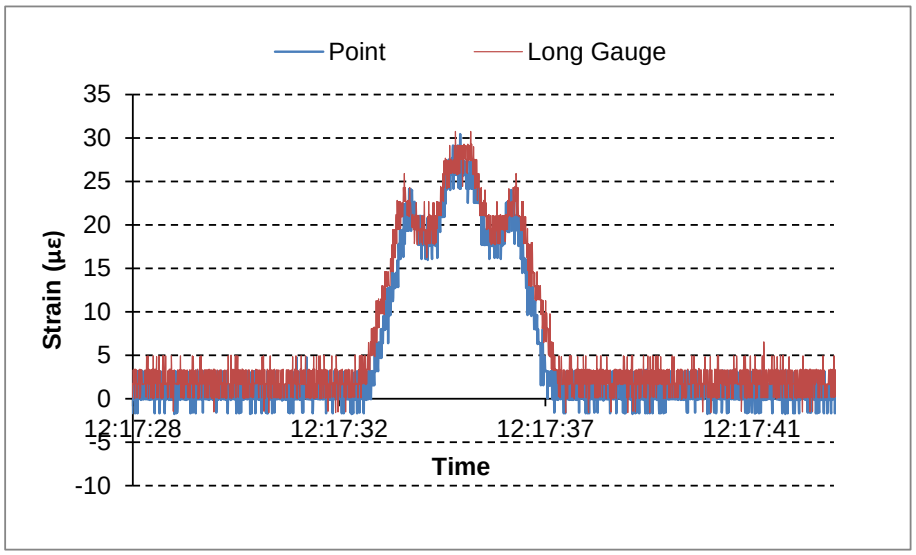

Figure 19. Deformation during the dynamic load test.

As can be seen, the there is a high degree of fit between the results obtained by both sensors. The maximum difference between the readings of both types during the dynamic test is 1.4 με, or 4.6 % of the measured increase in deformation. The difference in the measurements is clearly very small.

5. Conclusions

This paper describes the behavior and singularities of point and long-gage FBG strain sensors.

The behaviors of point and long gage sensors were compared in testing a concrete specimen and concrete column under compression. One point and one long-gage sensor were fitted to a concrete railway bridge to measure strain during static and dynamic load tests. As concrete is a heterogeneous material, a long-gage sensor was chosen for this application.

However, due to the singularities of the bridge under study: a) the proximity of an aggressive environment (sea) and b) a precast prestressed beam bridge in which the lower fiber was expected to be under compression during the tests (which closely imitates the possibility of cracks forming), the use of an additional point sensor was considered to compare its results to those of the long-gage sensor.

The sensors gave similar results in both the static and dynamic tests. Point sensors were used for this application due to their ease of installation, to avoid drilling into the structure to avoid exposure to the surrounding aggressive environment, and to reduce the cost of the monitoring system.

It can thus be concluded that point sensors can be used in special situations to measure strains on concrete elements, for example when it can be ensured that the concrete element will remain under compression and that cracking will not develop.

Acknowledgements

The authors wish to express their gratitude for the assistance received from the UTE ALTEA LINEA 9 company and also to the engineers Eduardo Luengo, Salvador Ivorra Chorro and David Bru Orts.